Synchronized Dynamic Induction Control
An Experimental Investigation

Van Vondelen, A. A.W.; Van Der Hoek, D. C.; Navalkar, S. T.; Van Wingerden, J. W.

DOI
10.1088/1742-6596/2767/3/032027

Publication date
2024

Document Version
Final published version

Published in
Journal of Physics: Conference Series

Synchronized Dynamic Induction Control: An Experimental Investigation

Journal of Physics: Conference Series **2767** (2024) 032027 doi:10.1088/1742-6596/2767/3/032027

Synchronized Dynamic Induction Control: An Experimental Investigation

AAW van Vondelen[1], DC van der Hoek[1], ST Navalkar[2], JW van Wingerden[1]

[1]Delft Center for Systems and Control, Delft University of Technology, Mekelweg 2, 2628 CD Delft, The Netherlands
[2]Siemens Gamesa Renewable Energy, Prinses Beatrixlaan 800, 2595 BN The Hague, The Netherlands

E-mail: A.A.W.vanVondelen@tudelft.nl

Abstract. Wind turbines in farms face challenges such as reduced power output and increased loading when their rows align with the wind direction—a phenomenon known as the wake effect. To address this issue, dynamic induction control has been proposed, which involves dynamically adjusting the induction of upstream turbines to enhance the mixing of the wake with the free stream. As a continuation of this method, downstream turbines could potentially leverage the periodic structure in the upstream turbines' wake to improve power production further downstream by synchronizing their dynamic induction control actions. This study investigates the potential of such an approach using a three-turbine scaled setup in a wind tunnel. The findings reveal that synchronization not only improves wake mixing downstream but also results in a substantial power gain on the synchronizing turbine, suggesting potential for a synchronization controller.

1. Introduction

In the construction of wind farms, a substantial amount of costs is saved compared to installing wind turbines individually, such as maintenance, installation, and cabling expenses. However, by placing turbines together, negative effects occur when the wind direction aligns with a row of turbines, a phenomenon commonly referred to as the wake effect [1]. As a result of the upstream turbines' wake, downstream turbines receive a turbulent, low-velocity wind field, which negatively impacts their power production and fatigue life. This scenario is commonly optimized in farm layouts, but it is estimated that still a large amount of power is lost due to these effects [2].

Control solutions have been proposed that attempt to mitigate these effects to improve production without compromising other aspects such as increased fatigue or actuator damage. These methods commonly optimize the farm as a whole, instead of the conventional approach of individual turbine control. This field is referred to as wind farm control [1].

One popular method, which is already implemented commercially by industry, uses yaw misalignments to redirect the wake [3,4]. However, while the wake is redirected from downstream turbines, it can still affect others, leaving potential for further optimization. This led researchers to find methods that promote wake mixing such that the wake dissipates faster.

The first of these wake-mixing methods was Dynamic Induction Control (DIC), which mixes the wake with the free stream wind by changing the induction [5]. This induction variation can be

accomplished by either changing the blade pitch or generator torque, thereby yielding faster and slower-moving vortices in the wake which interact and promote faster wake recovery. Initially, a computationally heavy adjoint-based model-predictive control approach was used to determine the optimal control action, yielding notable increases in farm-level power output [6]. However, due to the complexity of the method, practical implementation was challenging. As such, Munters and Meyers [7] heavily simplified the controller to a simple open-loop sinusoidal control action, referred to as periodic DIC, which achieved a lesser but still significant power increase.

Such an elegant solution to the wake effect caught the attention of other researchers who performed experimental studies and confirmed the power increases [8]. Another experiment, investigating the flow using particle image velocimetry, showed similar potential, as downstream power increased. However, no collective power gain was found due to actuation losses on the first turbine, which could largely be attributed to the smaller scale and sharper C_P curve of these machines [9]. Nevertheless, these studies underline the importance of continuing the investigation in improving existing and deriving novel wind farm control methods.

A method related to periodic DIC was proposed recently called Dynamic Individual Pitch Control (DIPC), which similarly involves dynamical variations [10]. The key difference is that DIPC applies a lag to the control action of each successive blade instead of a collective action, yielding a helical shape in the wake. Both these methods are commonly referred to as the 'pulse' and 'helix', respectively, referring to their characteristic wakes.

An open challenge remains the loads increase due to the actuation, where it appears that DIPC is favored over periodic DIC, because it suffers from strong tower loading and power oscillations, complicating practical implementations [11]. Between the two DIPC variants, clockwise (CW) and counter-clockwise (CCW), CCW shows a stronger power increase, while CW is favored for lower pitch bearing damage [12]. Nevertheless, these methods are still in active development and interesting control solutions may overcome these challenges.

In particular, wake-mixing methods have been studied primarily from an upstream perspective, and literature on wake-mixing control of waked, downstream, wind turbines is scarce. A recent study proposed an algorithm to synchronize the downstream control action with the incoming periodic wake to reduce the required actuation amplitude and decrease the pitch bearing damage [13]. Another paper demonstrated the effect of applying a phase shift when employing the helix approach on both the upstream and downstream wind turbines, where a performance increase or decrease was observed, depending on the selected phase offset [14].

For periodic DIC, similar power gains as mentioned in Korb et al. [14] may also be expected. As such, this study investigates the effect of a phase shift on the total power production of a three-turbine wind farm experimentally, where the contributions are presented as follows:

(i) Characterization of the effect of synchronized periodic DIC on the production of a three-turbine array for different phase shifts.

(ii) Derivation of a relationship between thrust and power for synchronized periodic DIC.

The remainder of this paper is organized as follows. Section 2 introduces periodic DIC, and the synchronization methodology is discussed in Section 3. The experimental setup is discussed in Section 4. Section 5 presents the experiment results, including analyses, and finally conclusions are drawn in Section 6.

2. Introduction to Dynamic Induction Control

This section provides an introduction to periodic DIC, including some considerations in terms of controller settings and synchronization methodology. Here, the control strategy for periodic DIC is adopted from [8], where blade pitch is used to vary the thrust, and thereby induction. The pitch signal, composed of a sinusoid, is defined by an amplitude, a phase, and a frequency.

The latter property is governed by the Strouhal number, a dimensionless number used in fluid dynamics to characterize the oscillating flow behavior around an object in a fluid stream:

$$St = \frac{f_e D}{U_\infty}, \tag{1}$$

where f_e is the excitation frequency in Hertz, D is the rotor diameter in meters, and U_∞ is the free stream wind speed in meters per second. The Strouhal number ensures the periodic DIC pitch settings can be scaled between different turbine sizes and wind speeds. Generally, an St between 0.2-0.4 is optimal for wake mixing, and experimental studies presented excellent results for periodic DIC with $St = 0.25$ [7], hence adopted in this work.

Upon selecting St and a pitch amplitude, usually no larger than 5-6 degrees due to physical constraints, a collective pitch actuation signal u_{c1} for turbine 1 (T1) can be constructed:

$$u_{c1} = A_{c1} \sin(f_{e1} 2\pi t), \tag{2}$$

where A_{c1} denotes the amplitude. A similar pitch signal is defined for T2:

$$u_{c2} = A_{c2} \sin(f_{e2} 2\pi t + \varphi_2). \tag{3}$$

The difference between Eq. (2) and Eq. (3) is the phase shift φ_2 added to the control action, which is incremented in the experiment to study the effect of in- to out-of-phase synchronization. Note that for synchronization $f_{e2} = f_{e1}$ is required, and for simplicity we also select $A_{c2} = A_{c1}$.

3. Synchronization methodology

This section discusses the methodology of synchronized periodic DIC. In such an approach, the upstream turbine operates using conventional DIC settings and is unaltered. The focus is now diverted to the downstream turbine, which must adapt the phase of its control action to exploit the periodic structure in the wake.

The synchronization idea originates from the presence of a characteristic periodic thrust variation found on the actuating turbine at the excitation frequency as a result of the collective pitch action of periodic DIC. This frequency is also present on the downstream turbine's thrust even though they employ baseline greedy control [11]. Such thrust variations imply that the wake sustains this periodic structure and transfers it to the downstream turbine as well affecting its thrust similarly albeit with lesser magnitude.

As such, a periodic DIC response with equal magnitude as the upstream's could potentially be obtained by slightly amplifying the thrust with the same frequency through a low-amplitude DIC action, alleviating the downstream turbine's pitch bearings. Or, the periodic thrust may be attenuated by actuating with a DIC action at the same frequency but out-of-phase, which may improve downstream turbine fatigue life, or enhance wake mixing further. Any phase shift in between may also provide interesting results, which are also examined in this work.

In summary, in-phase synchronization at the same frequency as the upstream turbine is expected to *amplify* the periodic response of the downstream turbine, which is then composed partly of the response to the wake and partly of its own pitching. Out-of-phase synchronization is expected to *reduce* the magnitude of the periodic thrust caused by the wake when actuated by the downstream turbine with the same frequency.

To study synchronization in an experimental setting, two methods can be evaluated. In the first, a phase shift $\Delta\theta_r$ of the response is used, which is defined here as the difference between the response on T2 actuated by the wake of T1, $y_{T2,w}$, and the response to the control action of T2, $y_{T2,c}$. If the responses are in phase, the resulting response will be increased in magnitude, in ideal conditions. If out of phase, the resulting response will be reduced, since they cancel:

$$\Delta\theta_r = \angle y_{T2,c} - \angle y_{T2,w}. \tag{4}$$

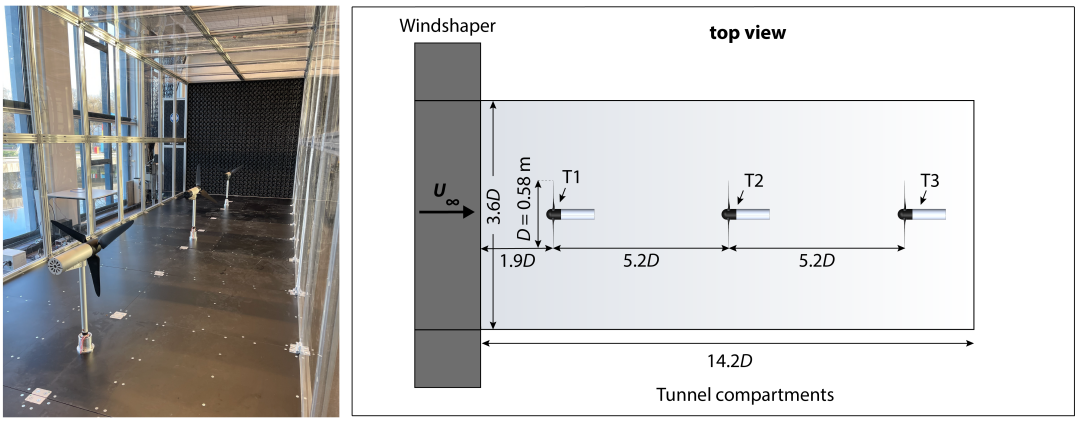

Figure 1: Wind AI Lab setup. Left: picture of the wind tunnel (in a different setup, for illustrative purposes). Right: top view schematic describing the setup used in this experiment.

In the second approach, a control phase shift is used, which is defined as the difference between the control signal of T2 with respect to T1:

$$\Delta\theta_c = \angle u_{c2} - \angle u_{c1}. \tag{5}$$

The first approach Eq. (4) requires an online estimator to differentiate between the responses and subsequently quantify their respective phase angles while the latter approach Eq. (5) is more straightforward to implement since all information is already available. However, environmental uncertainties such as small variations in wind speed invalidate the found optimal phase shift. As such, it is not possible to quantify an optimal phase shift or synchronized control strategy. Further research in estimation and control methods is required to synthesize such an approach (see e.g. for the Helix approach [13]). However, if a phase sweep of a full period is performed, a trend in produced power and thrust may be revealed, where low magnitude thrust indicates out-of-phase synchronization and high magnitude thrust indicates in-phase synchronization, allowing the deduction of a relation. Therefore, the latter approach is suitable to realize contributions (i) and (ii) and hence adopted in this experiment.

4. Experimental Setup

Upon determining the methodology in the previous section, the experimental setup for evaluating the synchronized control strategy is presented here. A description of the wind tunnel, wind turbine, and wind turbine control system is given, after which the test cases are determined.

4.1. Wind Tunnel

The experiments were performed in the Wind AI Lab, a new modular TU Delft testing facility for wind experiments [15]. The tunnel is located in a larger open space and the tunnel itself is composed of modular components with inner dimensions of 2.1x2.1x0.75m, such that its length can be varied easily. To generate flow, a WindShape[1] is controlled – an ensemble of small fans commonly used for drone testing that can reach a free stream velocity of up to 15 m/s [16]. Each module consists of two counter-rotating fans that can be controlled individually, allowing the creation of complex wind fields, such as gusts or sweeps.

In this work, all fans are given a constant pulse-width modulated (PWM) signal of 33% creating a wind field with a mean velocity of 5 m/s at hub height with an average turbulence

[1] https://windshape.com/

intensity of around 5%. A total of 11 modular components are connected where the turbines are mounted in components 2, 6, and 10, such that a spacing of approximately 5D is achieved. Figure 1 shows an image of the wind tunnel along with a schematic of the experimental setup.

4.2. Wind Turbine

The machines used in this experiment are three MoWiTo-0.6 scaled three-bladed wind turbines developed at Oldenburg University [17] (see Figure 2a). Each turbine is equipped with a generator for torque control, a collective pitch control system, and a rotor with diameter 0.58 m.

Since the scaled turbines have such a small rotor, it can be derived from Eq. (1) that f_e becomes quite large while keeping St constant. For example, compared to a modern wind turbine with a rotor diameter of 200 m, the actuation frequency required for the helix is approximately 345x higher requiring significant actuator bandwidth and potentially causing more loads. The amount of cycles increases which increases the damage-equivalent load, which is a function of cycles and amplitude.

Several measurements are available from the scaled turbines, including pitch angle, rotational speed, and generator current. Strain gauges were installed at the turbine's tower base to measure the turbine's fore-aft strain and are used to calculate the thrust (see Figure 2a). Control commands and measurements were exchanged with the wind turbine and computer using a dSPACE MicroLabBox[2], where a sampling frequency of 2 kHz was used.

In earlier work, the steady-state aerodynamic coefficients of the turbines, C_{P_e}, and C_T, the electrical power, and thrust, respectively, were determined [9]. A tip-speed ratio (TSR) of 5.5 and a collective pitch angle of 10 deg were found optimal for maximum power generation in the below-rated wind speed region when applying DIC. These coefficients are displayed in Figure 2b, where it can be observed that a small deviation from the optimal pitch angle can already result in a substantial loss of power. This implies that employing dynamic pitch strategies may result in significant power losses on the actuating scaled turbine, while in commercial turbines this is not expected due to flatter C_P curves. Hence, note that the chosen pitch angle of 10 deg does not yield the highest C_{P_e}, but is chosen as it is the center of the plateau, allowing the turbine to be in high C_{P_e} regions regardless of pitching around this value with DIC. Also, the controller gain K was determined in the earlier work [9], as the scaled turbines are torque-controlled using conventional $K\omega^2$ control, where ω denotes the rotational velocity.

4.3. Experiments

Recall from the methodology that Eq. (5) is adopted to study the effect of a phase shift on the power and thrust of the downstream turbines. As it is not possible to quantify the exact phase of the helix wake when it interacts with the downstream turbine, a parameter sweep, which increments phase steps, may reveal a trend in power production and thrust. Such a sweep is conducted by initiating a cycle where several cases are evaluated succeeding each other. The cycle is started by initiating a wind field using the WindShape and controlling the turbines at their greedy optimum. Then, the cases are performed: each measurement lasting 60 seconds with a 15-second pause (baseline control on T2) in between. After a baseline periodic DIC case, the first synchronized periodic DIC test case is evaluated with a 0 deg phase shift. The next case's phase is shifted by 30 degrees until completing the period at 330 deg, where the full experiment cycle is repeated a total of four times. Table 1 summarizes the evaluated cases.

5. Results

This section discusses the key findings derived from four experiment cycles, focusing on the total power production of T2 and T3 combined, individual turbine performances, and their

[2] https://www.dspace.com/en/inc/home/products/hw/microlabbox.cfm

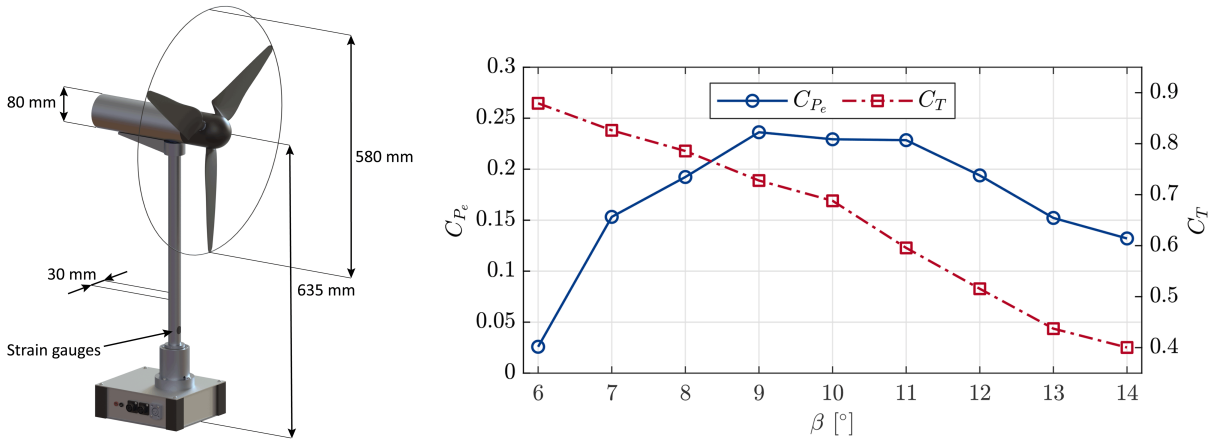

(a) Illustration of the MoWiTo-0.6 scaled wind turbine and its dimensions and strain gauge location.

(b) Characterisation of the aerodynamic coefficients of the MoWiTo for the optimal tip-speed ratio of 5.5. Note the sharp decline of C_{P_e} for a slight deviation from the optimal pitch angle.

Figure 2: Relevant parameters of the MoWiTo-0.6 (Figures adapted from [9]).

Table 1: Summary of the evaluated cases. BL denotes baseline.

Case	**T1**	**T2**	**T3**
BL periodic DIC	Periodic DIC	Greedy	Greedy
Test Cases	Periodic DIC	Sync periodic DIC + 0:30:330 deg	Greedy

interactions. Figure 3 illustrates the combined average power production $\mu(\mathcal{P})$ across various control offsets. The baseline periodic DIC production is indicated by a horizontal dashed line for reference. Notably, considerable performance improvements are observed for different phase offsets compared to the baseline periodic DIC case. In experiment cycle 1, a clear peak is observable between 120 and 180 degrees where the combined production exceeds the baseline production indicated by the dashed horizontal line. At other phase offsets, the combined production is lower, implying that periodic DIC cannot simply be applied to a downstream turbine without considering the phase of the wake of the upstream turbine. In the other experiment cycles similar observations can be made, showing distinct areas with high production and distinct areas with lower production demonstrating potential for a synchronized DIC approach maintaining the optimal phase offset.

It can further be observed that between the four cycles, there is no consistency in optimal offset, which can be attributed to the earlier mentioned uncertainty regarding the actual phase at which the wake interacts with the downstream turbine. Slight variations in wind speed between experiment cycles may induce phase shifts, resulting in different outcomes. Nevertheless, identifiable optimal and suboptimal regions with respect to phase offset persist, exhibiting relatively smooth transitions across the cases.

Proceeding, the individual power production of T2 is studied in conjunction with the standard deviation of the thrust $\sigma(T)$ in Figure 4. Interestingly, for several phase offsets, a performance increase compared to the baseline periodic DIC case is found at T2, a noteworthy result considering the sharp C_P curve of the scaled turbines (Figure 2b)—a deviation from the optimal pitch results in a much more significant power production drop compared to utility-scaled turbines. This observation suggests that synchronized periodic DIC may yield better energy extraction for downstream turbines compared to a greedy control approach and better

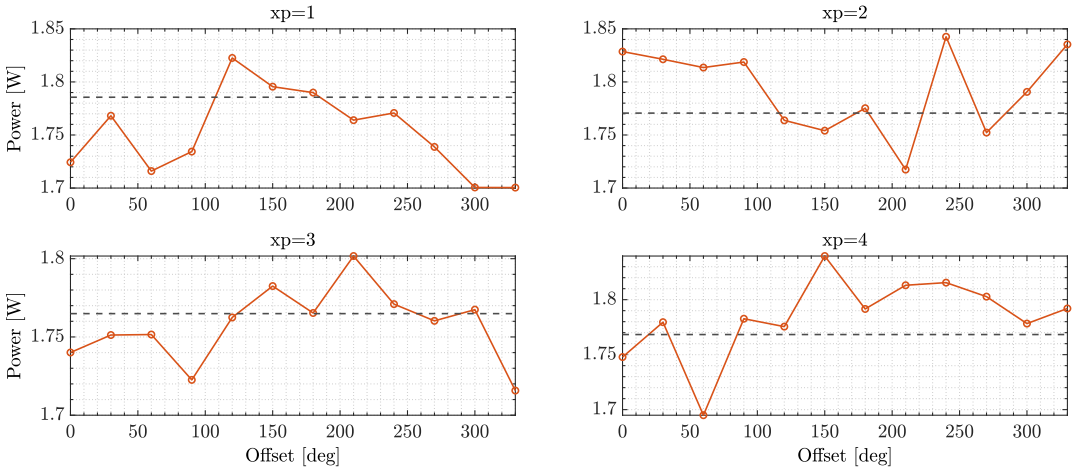

Figure 3: Power production of T2 and T3 combined across different control offsets, for experiments 1 to 4. Each figure displays the results obtained in the respective experiment cycle. The baseline periodic DIC case is indicated by horizontal dashed lines.

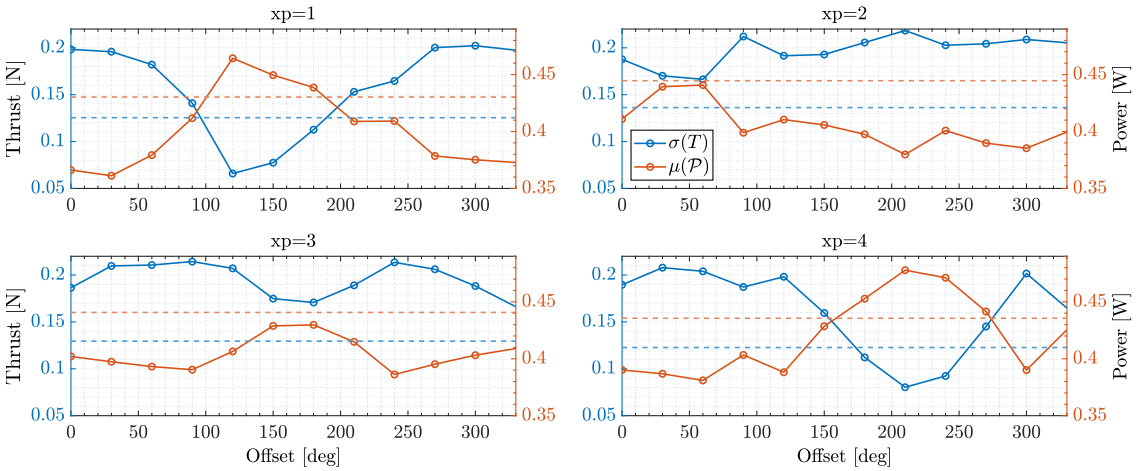

Figure 4: Power production of T2 overlaid with the thrust, for experiments 1 to 4. Each figure displays the results obtained in the respective experiment cycle. The baseline periodic DIC case is indicated by horizontal dashed lines.

performance may be expected on utility-scale turbines. Further note that T2 has a much lower contribution to the combined power than T3. This can be explained by the strong velocity deficit still present from T1, and the actuation losses resulting from applying DIC on T2. T3 benefits most from the DIC on T1 and T2 and therefore sees a large production.

Now comparing the standard deviation of the thrust with the power reveals an interesting inverse relation. A high gain is obtained on the synchronizing turbine when thrust variations are low, which suggests an out-of-phase control action is optimal for maximizing power on T2.

Further investigation in the power spectra of the thrust of T2, where the highest and lowest power production are compared in Figure 5, suggests a similar conclusion. The magnitude at f_e is lower during the highest power production, while the magnitude during low power production is higher. Also, the $1P$ frequency shifts upward during higher power production.

In contrast, the power production of T3 overlaid with the standard deviation of the thrust of T2 in Figure 6 shows no discernible relation. The smaller absolute differences in maximum and

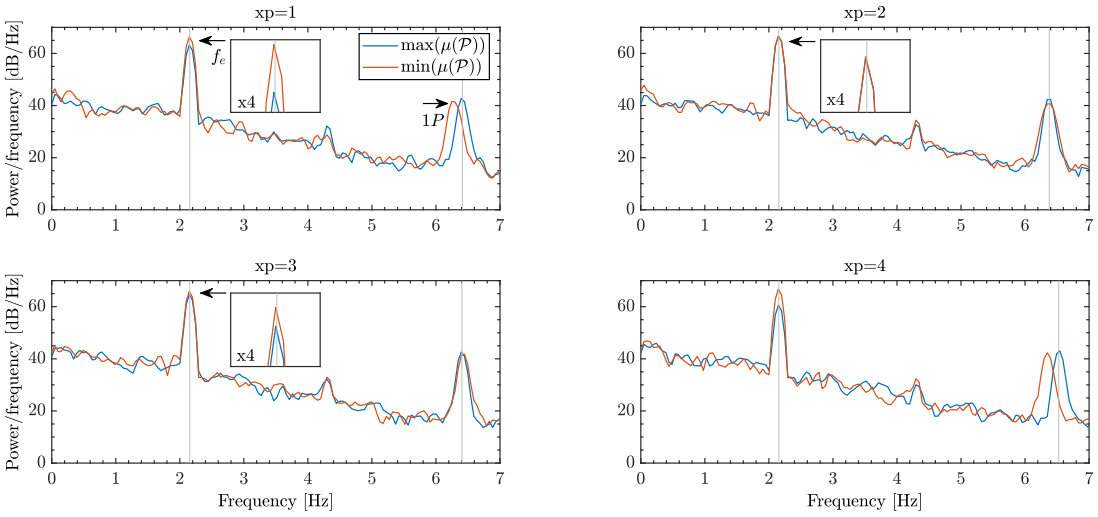

Figure 5: Comparison of the spectra of the thrust of T2 between the case with lowest and highest power, for experiments 1 to 4. Each figure displays the results obtained in the respective experiment cycle.

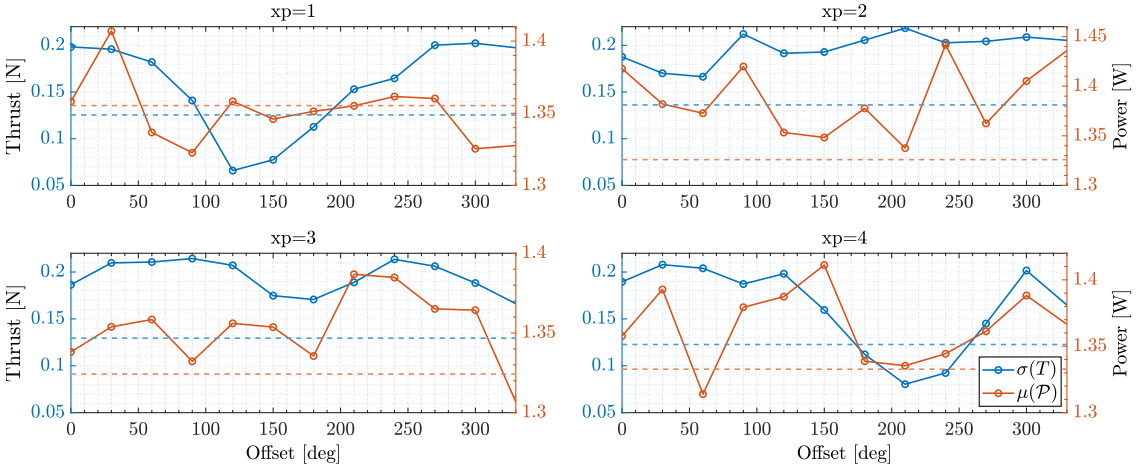

Figure 6: Power production of T3 overlaid with the thrust of T2, for experiments 1 to 4. Each figure displays the results obtained in the respective experiment cycle. The baseline periodic DIC case is indicated by horizontal dashed lines.

minimum power production suggest that synchronized periodic DIC may play a more critical role for the synchronizing turbine (T2) than the one further downstream (T3).

Finally, an inspection of the relation between the thrust on T2 with the total power production on T2 and T3 is performed in Figure 7. Here, it is discernable that, although less strong (Table 2), the inverse relation persists for the combined power production, confirming the suitability of an out-of-phase, or load-rejecting synchronization controller on T2.

A subsequent investigation of the correlation between the standard deviation of the thrust on T2 and the power of T2 and T3 is summarized in Table 2. It is observed that for T2, the correlations approach -1, indicating an inverse relationship. For T3, the correlations imply no significant relationship with the thrust on T2. However, for the combined production, similar to T2, an inverse relation exists, where a low thrust on T2 implies a high power gain.

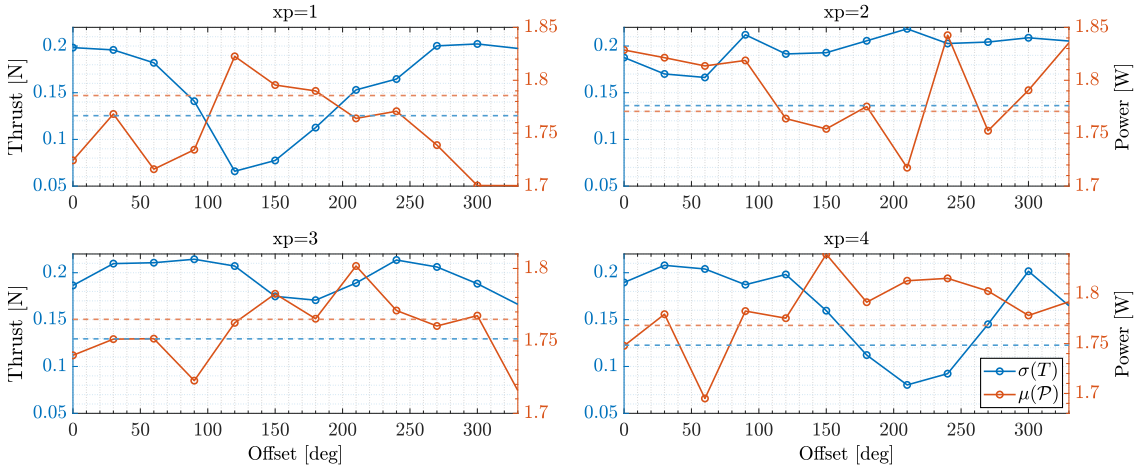

Figure 7: Power production of T2 and T3 combined overlaid with the thrust of T2, for experiments 1 to 4. Each figure displays the results obtained in the respective experiment cycle. The baseline periodic DIC case is indicated by horizontal dashed lines.

Table 2: Overview of the correlation of the mean power of T2, T3 and T2 + T3 combined, with the standard deviation of the thrust on T2.

XP	**T2**	**T3**	**T2 + T3**
1	-0.97	0.09	-0.83
2	-0.96	-0.06	-0.54
3	-0.90	0.19	-0.44
4	-0.98	0.42	-0.61

6. Conclusion

To conclude, this study investigated experimentally the effects on power production by synchronizing the dynamic induction control action of the downstream turbine with the upstream turbine's control action. The investigation involved introducing a phase shift to the downstream turbine's control action, examining both in-phase and out-of-phase synchronization. The findings demonstrated the possibility of achieving a substantial power gain over baseline periodic dynamic induction control within a three-turbine array under specific phase offsets.

Due to the nature of the experiment, the actual phase offset with respect to the incoming wake on the downstream turbine could not be estimated. Instead, the thrust was analysed, which in case of in-phase synchronization is maximum and in case of out-of-phase synchronization is minimum. Consequently, an inverse relationship was identified between thrust variations and power production. The highest power gain on turbine two even exceeded the baseline production, which is unusual considering the actuating turbine generally suffers a loss by deviating from the optimal pitch on the C_P curve. These findings suggest potential benefits from employing out-of-phase synchronization or a load rejection controller, which could potentially reduce thrust variations and enhance performance on the second turbine at the same time.

A relationship between the thrust of the second turbine and the power of the third turbine could not be established. However, the relation persisted for the combined production, although less strong. More extensive flow investigations conducting for example particle image velocimetry experiments or performing large-eddy simulations could provide insights into the fluid dynamics to explain the power and thrust relations found in this work. Further investigations may then unveil the potential of a load rejection controller or synchronization controller for the downstream

turbine, providing valuable insights for optimizing power production in multi-turbine arrays.

Acknowledgement
This work is part of the Hollandse Kust Noord wind farm innovation program where CrossWind C.V., Shell, Grow, Eneco and Siemens Gamesa are teaming up; funding for the PhDs was provided by CrossWind C.V. and Siemens Gamesa. We further acknowledge Wim Wien and Will van Geest for preparing the experimental setup.

References

[1] J. Meyers, C. Bottasso, K. Dykes, P. Fleming, P. Gebraad, G. Giebel, T. Göçmen, and J. W. van Wingerden, "Wind farm flow control: prospects and challenges," *Wind Energy Science*, vol. 7, no. 6, pp. 2271–2306, 2022.

[2] R. J. Barthelmie, K. Hansen, S. T. Frandsen, O. Rathmann, J. Schepers, W. Schlez, J. Phillips, K. Rados, A. Zervos, E. Politis, *et al.*, "Modelling and measuring flow and wind turbine wakes in large wind farms offshore," *Wind Energy*, vol. 12, no. 5, pp. 431–444, 2009.

[3] P. A. Fleming, P. M. Gebraad, S. Lee, J. W. van Wingerden, K. Johnson, M. Churchfield, J. Michalakes, P. Spalart, and P. Moriarty, "Evaluating techniques for redirecting turbine wakes using sowfa," *Renewable Energy*, vol. 70, pp. 211–218, 2014.

[4] Siemens Gamesa, "Siemens gamesa now able to actively dictate wind flow at offshore wind locations," 2019. https://www.siemensgamesa.com/en-int/newsroom/2019/11/191126-siemens-gamesa-wake-adapt-en.

[5] J. P. Goit and J. Meyers, "Optimal control of energy extraction in wind-farm boundary layers," *Journal of Fluid Mechanics*, vol. 768, pp. 5–50, 2015.

[6] W. Munters and J. Meyers, "An optimal control framework for dynamic induction control of wind farms and their interaction with the atmospheric boundary layer," *Philosophical Transactions of the Royal Society A: Mathematical, Physical and Engineering Sciences*, vol. 375, no. 2091, p. 20160100, 2017.

[7] W. Munters and J. Meyers, "Towards practical dynamic induction control of wind farms: analysis of optimally controlled wind-farm boundary layers and sinusoidal induction control of first-row turbines," *Wind Energy Science*, vol. 3, no. 1, pp. 409–425, 2018.

[8] J. A. Frederik, R. Weber, S. Cacciola, F. Campagnolo, A. Croce, C. Bottasso, and J. W. van Wingerden, "Periodic dynamic induction control of wind farms: proving the potential in simulations and wind tunnel experiments," *Wind Energy Science*, vol. 5, pp. 245–257, 2020.

[9] D. van der Hoek, J. Frederik, M. Huang, F. Scarano, C. Simao Ferreira, and J. W. van Wingerden, "Experimental analysis of the effect of dynamic induction control on a wind turbine wake," *Wind Energy Science*, vol. 7, no. 3, pp. 1305–1320, 2022.

[10] J. A. Frederik, B. M. Doekemeijer, S. P. Mulders, and J. W. van Wingerden, "The helix approach: Using dynamic individual pitch control to enhance wake mixing in wind farms," *Wind Energy*, vol. 23, no. 8, pp. 1739–1751, 2020.

[11] J. A. Frederik and J. W. van Wingerden, "On the load impact of dynamic wind farm wake mixing strategies," *Renewable Energy*, 2022.

[12] A. A. W. van Vondelen, S. T. Navalkar, D. R. H. Kerssemakers, and J. W. van Wingerden, "Enhanced wake mixing in wind farms using the helix approach: A loads sensitivity study," in *2023 American Control Conference (ACC)*, (San Diego, California, USA), AACC, 2023.

[13] A. A. W. van Vondelen, J. Ottenheym, A. K. Pamososuryo, S. T. Navalkar, and J. W. van Wingerden, "Phase synchronization for helix enhanced wake mixing in downstream wind turbines," in *2023 IFAC World Congress*, 2023.

[14] H. Korb, H. Asmuth, and S. Ivanell, "The characteristics of helically deflected wind turbine wakes," *Journal of Fluid Mechanics*, vol. 965, p. A2, 2023.

[15] "TU Delft opens globally unique wind tunnel," 9 2022. https://www.tudelft.nl/en/2022/3me/news/tu-delft-opens-globally-unique-wind-tunnel.

[16] F. Noca, G. Catry, N. Bosson, L. Bardazzi, S. Marquez, and A. Gros, "Wind and weather facility for testing free-flying drones," in *AIAA Aviation 2019 Forum*, p. 2861, 2019.

[17] J. Schottler, A. Hölling, J. Peinke, and M. Hölling, "Design and implementation of a controllable model wind turbine for experimental studies," in *Journal of Physics: Conference Series*, vol. 753, p. 072030, IOP Publishing, 2016.